JACS
JOURNAL OF THE AMERICAN CHEMICAL SOCIETY
Article
pubs.acs.org/JACS

Direct Observation of Very Large Zero-Field Splitting in a Tetrahedral $Ni^{II}Se_4$ Coordination Complex

Shang-Da Jiang,[†,⊥,▽] Dimitrios Maganas,[‡,▽] Nikolaos Levesanos,[∥] Eleftherios Ferentinos,[∥] Sabrina Haas,[†] Komalavalli Thirunavukkuarasu,[§] J. Krzystek,[§] Martin Dressel,[†] Lapo Bogani,*[,†,#] Frank Neese,*[,‡] and Panayotis Kyritsis*[,∥]

[†]1. Physikalisches Institut, Universität Stuttgart, Pfaffenwaldring 57, D-70550, Stuttgart, Germany

[‡]Max-Planck-Institut für Chemische Energiekonversion, Stiftstrasse 34-36, D-45470 Mülheim an der Ruhr, Germany

[∥]Laboratory of Inorganic Chemistry, Department of Chemistry, National and Kapodistrian University of Athens, Panepistimiopolis, Athens, 157 71 Greece

[§]National High Magnetic Field Laboratory, Florida State University, Tallahassee, Florida 32310, United States

Supporting Information

ABSTRACT: The high-spin (S = 1) tetrahedral Ni^{II} complex [Ni{$^iPr_2$P(Se)NP(Se)$^iPr_2$}$_2$] was investigated by magnetometry, spectroscopic, and quantum chemical methods. Angle-resolved magnetometry studies revealed the orientation of the magnetization principal axes. The very large zero-field splitting (zfs), D = 45.40(2) cm^{-1}, E = 1.91(2) cm^{-1}, of the complex was accurately determined by far-infrared magnetic spectroscopy, directly observing transitions between the spin sublevels of the triplet ground state. These are the largest zfs values ever determined—directly—for a high-spin Ni^{II} complex. *Ab initio* calculations further probed the electronic structure of the system, elucidating the factors controlling the sign and magnitude of D. The latter is dominated by spin−orbit coupling contributions of the Ni ions, whereas the corresponding effects of the Se atoms are remarkably smaller.

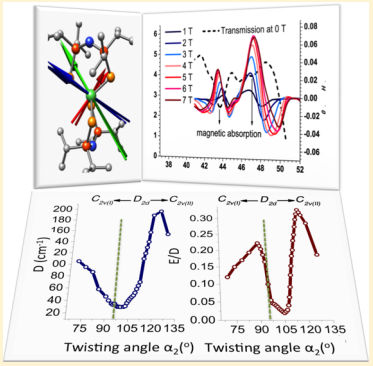

INTRODUCTION

The discovery, in the early 1990s, of clusters of paramagnetic metal ions exhibiting slow relaxation of the magnetization at low temperature, since termed single-molecule magnets (SMMs), has been a hallmark in the field of molecular magnetism.[1] In a simple approximation,[2] the energy barrier for the reversal of magnetization of a SMM amounts to $|D|S^2$, with D being the axial component of the zero-field splitting (zfs) tensor,[3] and S the total spin of the ground state. Extensive studies on SMMs during the last two decades have established that when intramolecular exchange interactions dominate, the principal factors governing their magnetic behavior are the electronic spin and the zfs of the individual metal ions, which, combined through spin−spin exchange, yield the total spin (S) and the overall zfs of the cluster. Although ferromagnetic exchange interactions between the single paramagnetic sites of a cluster, promoted by appropriate bridging ligands, can lead to large S values, the overall zfs of metal clusters is usually remarkably small, because it is difficult to precisely orient the easy axes of the spin centers.[2,4] For that reason, properties akin to those of SMMs have been recently sought—and found—in mononuclear complexes of lanthanides and actinides[5] or d-metal ions,[6] which can exhibit much larger zfs, compared with that of metal clusters. Thus, in order to design a mononuclear SMM, it is important to develop methods to accurately determine the zfs of mononuclear metal complexes, in order to understand in depth the factors controlling its sign and magnitude. Small zfs of multinuclear clusters can be accurately determined by high-frequency and -field electron paramagnetic resonance (HFEPR) spectroscopy and related techniques.[4,7] This is not always the case for mononuclear metal complexes,[8,9] the zfs magnitude of which[6,8,9] frequently exceeds the frequencies available in HFEPR (generally below ∼1 THz or 33 cm^{-1})[10] and thus can only be determined by indirect methods such as magnetometry[11] or magnetic circular dichroism (MCD) spectroscopy.[12] An additional spectroscopic technique, namely far-infrared magnetic spectroscopy (FIRMS), can provide a direct way of determining the magnitude of zfs,[13] but it has not been employed as extensively as magnetometry (*vide infra*). In this work, FIRMS was indeed employed to directly determine the zfs of a tetrahedral Ni^{II} complex, [Ni{$^iPr_2$P(Se)NP(Se)$^iPr_2$}$_2$] (**1**) (Figure 1a),[14] the sign and magnitude of which ($D \sim 45$ cm^{-1}) exceeds the limit directly detectable by HFEPR. Although, as expected,[2] complex **1** does not exhibit SMM properties due to its integer S (= 1) and positive D (*vide infra*), two mononuclear Ni^{II} complexes showing negative D,[15a,b] along with a Ni(I) complex,[15c] have

Received: June 29, 2015
Published: September 9, 2015

DOI: 10.1021/jacs.5b06716
J. Am. Chem. Soc. 2015, 137, 12923−12928

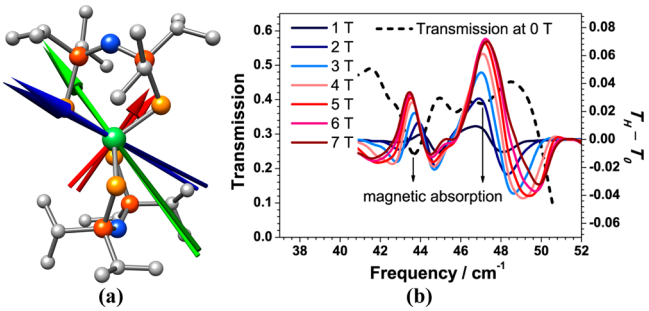

Figure 1. (a) Visualization of the molecular structure of **1** along with the experimentally determined (green, blue and red arrows) magnetization (x, y, z) principal axes and the calculated (light green, blue and red arrows) zfs tensor (x, y, z) components, in the crystallographic molecular frame. Atoms color coding: Ni (green), Se (orange), P (brown), N (blue), C (gray). (b) FIR transmission spectra at 5 K of complex **1** in the presence or absence of external magnetic fields. The dashed line is the FIR spectrum in the absence of field corresponding to the left vertical axis. The colored lines are the spectra at various fields (T_H transmissions) normalized with respect to the zero-field (T_0) one, corresponding to the right vertical axis.

recently been shown to do so. The origins of the zfs of complex **1** were subsequently investigated in detail via *ab initio* quantum chemical calculations of the electronic structure of the complex.

DISCUSSION

The zfs is often expressed by the first two terms in the spin Hamiltonian presented in eq 1:

$$\hat{H} = D\left[\hat{S}_z - \frac{S(S+1)}{3}\right] + E(S_+^2 + S_-^2) + \mu_B \vec{B}\,\mathbf{g}\hat{S} \quad (1)$$

in which D and E are its axial and rhombic components, respectively, and the last term denotes the Zeeman effect (see also the Supporting Information). In the absence of magnetic field, the action of $\hat{H}$ on the $S = 1$ system is to split the spin multiplet into three sublevels, denoted as $|+\rangle$, $|-\rangle$, and $|0\rangle$, as visualized in Scheme S1. There are two possible cases, $D > 0$ and $D < 0$, referred to as easy-plane and easy-axis anisotropy, respectively. In each case, at zero field, the sub-THz or THz wave radiation-induced transitions between all three levels are allowed.[3] Magnetometry and HFEPR have been intensively employed in studying high-spin, $S = 1$, Ni^{II} complexes of various geometries and coordination spheres.[16−18] Of particular importance are two recently reported Ni^{II} complexes of different geometry displaying extremely large zfs values, as indirectly estimated by HFEPR (trigonal bipyramidal, $D = -120$ to -180 cm^{-1}, $E = 1.6$ cm^{-1})[18e] and by magnetometry alone (trigonal pyramidal, $D = -200$ cm^{-1}).[18g] Only a range of D values has been estimated for the former by observing the $|+\rangle \rightarrow |-\rangle$ transition (red arrow, Scheme S1) amounting to $2|E|$.[18e] For Ni^{II} systems of tetrahedral coordination, MCD studies[12] together with empirical ligand-field theory analysis based on parameters extracted by nickel L-edge X-ray absorption spectroscopy[19] have provided estimates of large D values (44−76 cm^{-1}) for $[Ni(SPh)_4]^{2-}$ and the $[Ni(Cys)_4]^{2-}$ active site of Ni^{II}-substituted rubredoxin. Confirming this trend, magnetometry and computational methods have predicted very large D values for tetrahedral Ni^{II} complexes bearing dichalcogenidoimidodiphosphinato ligands.[20] Consistent with those observations, three complexes of the same type, namely $[Ni\{Ph_2P(S)NP(S)Ph_2\}_2]$,[21] $[Ni\{Ph_2P(O)NP(Se)Ph_2\}_2]$,[22] and **1**,[14] were investigated in this work by HFEPR up to 400 GHz (13 cm^{-1}) and 14.5 T and showed no resonances originating from an $S = 1$ system. Complex **1** was further studied at frequencies up to 700 GHz (23 cm^{-1}) and magnetic fields up to 35 T, and again proved to be silent. This observation is compatible with a large ($> \sim 25$ cm^{-1}) magnitude of D for this system. The failure to detect the $|+\rangle \leftrightarrow |-\rangle$ transition, as was the case for an easy-axis anisotropy type system,[18e] is a strong indication of a positive D for complex **1**, due to the fact that this transition would then involve the excited $|-\rangle$ and $|+\rangle$ magnetic sublevel states (Scheme S1), and therefore its observation would require elevated temperatures, at which spin relaxation renders the EPR response undetectable. It is thus clear that in order to accurately determine the magnitude of the zfs in the above tetrahedral Ni^{II} complexes and hence get insight into their magnetic and electronic properties, alternative experimental techniques are necessary. Our method of choice is FIRMS, also known as frequency domain magnetic resonance spectroscopy.[13] This method has been employed to directly probe magnetic transitions in Fe^{II} systems[23] as well as in certain multinuclear SMMs.[24] By the same approach, the magnitude of D has been determined for nickelocene (32 cm^{-1})[25] as well as for tetrahedral (13.3 cm^{-1}),[13a,26] octahedral (−10 cm^{-1}),[27] and pentacoordinated (15 cm^{-1})[28] Ni^{II} complexes.

The magnetization (M) of a powder sample of **1** as a function of temperature was investigated below 20 K at various static fields on a superconducting quantum interference device magnetometer. The M vs BT^{-1} plots (Figure S1) at magnetic fields B between 5×10^{-3} and 5 T are not superimposed, which is compatible with a system exhibiting large magnetic anisotropy. The magnetization value at 5 T in the whole temperature range is 0.34 μ_B, much smaller than the saturation value of an $S = 1$ system with $g = 2.2$. The small value of the magnetization provides evidence for easy-plane anisotropy. By fitting the magnetization function to the experimental data, the zfs and Landé parameters are determined to be $D = 43.4(2)$ cm^{-1}, $E = 2.6(1)$ cm^{-1} and $g_{iso} = 2.22(5)$, where the **g** tensor is constrained as isotropic to avoid overfitting. It should be stressed that negative values of D did not produce satisfactory fits.

A more direct and accurate approach to obtain the spin Hamiltonian parameters of complex **1** was provided by applying FIRMS. The zero-field far-infrared (FIR) spectrum at 5 K of **1**, shown in Figures 1b and S2, is rather broad, and assuming $D > 0$, it is expected to originate from the $|0\rangle \rightarrow |+\rangle$ and $|0\rangle \rightarrow |-\rangle$ magnetic transitions amounting to $|D|+|E|$ and $|D|-|E|$, respectively (Scheme S1)[3] as well as from vibrational ones.[26] The two types of signals can be distinguished by magnetic field, which could shift only the magnetic transitions (Figures 1b and S2). By normalizing the 5 K spectra at various magnetic field strengths with respect to the zero-field spectrum, two distinct bands at 43.50 and 47.31 cm^{-1} are clearly visible, which are significantly split and shifted in the presence of magnetic fields. Hence, based on the spectroscopic data of Figure 1a, the values of $|D| = 45.40(2)$ cm^{-1} and $|E| = 1.91(2)$ cm^{-1} are directly and accurately obtained. To the best of our knowledge, the D value of complex **1** is the largest ever reported for a metal complex based on studies by FIRMS[13,23−28] or by the recently developed analogous method frequency domain Fourier transform THz EPR spectroscopy.[29]

Taking also into account the fact that D is indeed positive (*vide infra*), these data justify the HFEPR silence of **1** and

DOI: 10.1021/jacs.5b06716
J. Am. Chem. Soc. 2015, 137, 12923−12928

reliably confirm the magnetometric estimates. The two bands shown in Figure 1a are significantly shifted as the field strength is varied up to 7 T (see also Figure S2). The dependence of the peak position on the field strength is nonlinear, an observation compatible with an $S = 1$ system exhibiting rhombic zfs. Fitting the field dependence of the transition positions into the spin Hamiltonian eq 1, a value of $g_{iso} = 2.18(2)$ was obtained, in good agreement with the one derived by the magnetization data.

The type of the magnetic anisotropy of **1** was further established by the temperature dependence of the FIR spectra. In a nutshell, for a system of easy-axis anisotropy, one of the two $|0\rangle \leftrightarrow |+\rangle$ and $|0\rangle \leftrightarrow |-\rangle$ transitions (blue arrows, Scheme S1) involves a pair of excited states, and hence its intensity would decrease rapidly at low temperatures, due to spin depopulation. On the other hand, in the case of easy-plane anisotropy, both transitions involve the ground state (Scheme S1), and therefore their intensity ratio would remain approximately constant at low temperature. The temperature dependence of the measured transition line intensity can be described by the magnitude of the magnetic permeability determined by the spectra fitting, as shown in Figure S3. The magnetic permeability data for both easy-axis and easy-plane anisotropy were simulated by using the same $|D|$ and $|E|$ values. The data presented in Figure S3 provide clear evidence that the system exhibits easy-plane magnetic anisotropy. Moreover, since **1** crystallizes in a *P*-1 space group and there is only one symmetrically independent molecule in the unit cell,[14] the orientation of the magnetization principal axes could be determined by angle-resolved magnetometry, i.e., magnetometric studies on oriented single crystals. This endeavor has been undertaken in an effort to probe magnetostructural correlations in lanthanide-based SMMs,[30] but it has not yet extensively applied to d-metal-based complexes. For that purpose, the angular dependence of the magnetic susceptibility was monitored by rotating a single crystal of **1** embedded on an L-shaped Cu−Be support,[30a] around the three orthogonal axes, at temperatures between 1.8 and 5 K (Figure S4). Strong anisotropy of the magnetization is observed for the rotation around the *x*- and *y*-axes, whereas with the *z*-axis rotation the magnetization is more isotropic and has a larger value. This observation strongly implies an easy-plane anisotropy, and the *z*-axis could be very close to the zfs hard axis. The susceptibility tensor in the experimental frame was extracted by simultaneously fitting the three rotation planes at the same temperature. The principal axes and the corresponding susceptibility are therefore the eigenvectors and eigenvalues of the susceptibility tensor. At 5 K, two of the principal values (0.07 and 0.06 emu mol^{-1}) are very close to each other and much larger than the third one (0.02 emu mol^{-1}), confirming that the system exhibits an easy-plane anisotropy. The orientation of the experimentally determined magnetization principal axes is shown in Figure 1a, where it can be seen that these axes are misoriented with respect to the crystallographic ones. For instance, the magnetic hard axis (red arrow, Figure 1a) deviates from the pseudo C_2 symmetry axis. Apparently, simple magnetostructural correlations cannot be made, and a more elaborate investigation of this observation is needed by quantum chemical calculations (*vide infra*).

The origin of zfs is generally two-fold: (a) spin−spin coupling (SSC) between the unpaired electrons, and (b) admixture of excited electronic states into the ground state of the complex via spin−orbit coupling (SOC).[9] Based on our experience, concerning accuracy and efficiency, a correlation of the experimentally determined zfs parameters with the electronic structure of the system under investigation is best performed by applying the "Master matrix" formalism[9] on the basis of state-averaged complete active space self-consistent-field (SA-CASSCF) wave functions and multireference second-order perturbation theory, e.g., second-order N-electron valence perturbation theory (NEVPT2) energies. In this formalism, the SOC and SSC effects are treated through diagonalization of the Born−Oppenheimer (BO) SOC and SSC operators, on the basis of triplet and singlet roots of the BO Hamiltonian (extended to treat all $m_s = S, S - 1, ..., -S$, components of a given relativistic many particle energy level). This protocol has been proven successful in treating magnetic systems containing both nondegenerate and degenerate ground states.[9]

The pseudotetrahedral $NiSe_4$ core of **1**[14] can be best described by assuming reference geometries of D_{2d} symmetry (Figure 2). This strategy has been proven valid in studying the

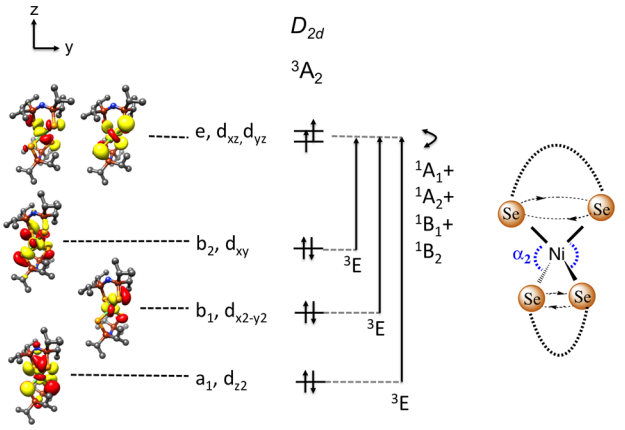

Figure 2. Left: The metal−d-based MO and term symbols (analyzed under approximate D_{2d} symmetry), arising from single excitations in the elongated tetrahedral complex **1**. The indicated orbital occupation pattern refers to the $^3A_2$ ground state. Right: a schematic representation of the twisting angle α_2.

structural and electronic properties of specific examples of $[M\{R_2P(X)NP(X)R'_2\}_2]$ type of complexes, M = Co,[31] Ni;[17,20,22] X = O, S, Se; R, R′ = Me, Ph, ^{i}Pr. As shown in Figure 2, under D_{2d} symmetry, the ground state of **1** is $^3A_2$, corresponding to the $a_1^2b_1^2b_2^2e^2$ electron configuration. For complexes bearing tetrahedral NiS_4[20] and NiS_2O_2[17,22] cores, it has been shown that the pseudo-Jahn−Teller (PJT) effect and/or molecular orbital relaxation effects can stabilize the ^3E ($b_2^1e^3$) states over the $^3A_2$ ($b_2^2e^2$) state, along the $D_{2d} \rightarrow C_{2v}$ interconversion pathway. However, this phenomenon is canceled out in the presence of bulky R peripheral groups (Ph or ^{i}Pr), which force complexes bearing symmetric NiS_4 cores, such as $[Ni\{R_2P(S)NP(S)R_2\}_2]$, R = Ph, ^{i}Pr, to retain their local D_{2d} symmetry.[20] Apparently, this seems to be also the case for complex **1**, and it is hence important to analyze its magnetic properties in terms of both first- and second-coordination sphere effects. As illustrated in Figure 3a and discussed in more detail elsewhere,[20,22] the symmetry-lowering interconversion pathway $C_{2v(I)} \rightarrow D_{2d} \rightarrow C_{2v(II)}$ is dominated by the twisting angle a_2 which, for complex **1**, is defined by the pairs of exo Se−Ni−Se angles (Figures 2 right, S5). Along this pathway, the $^3A_2$ ($b_2^2e^2$) ground state is expected to be unstable

DOI: 10.1021/jacs.5b06716
J. Am. Chem. Soc. 2015, 137, 12923−12928

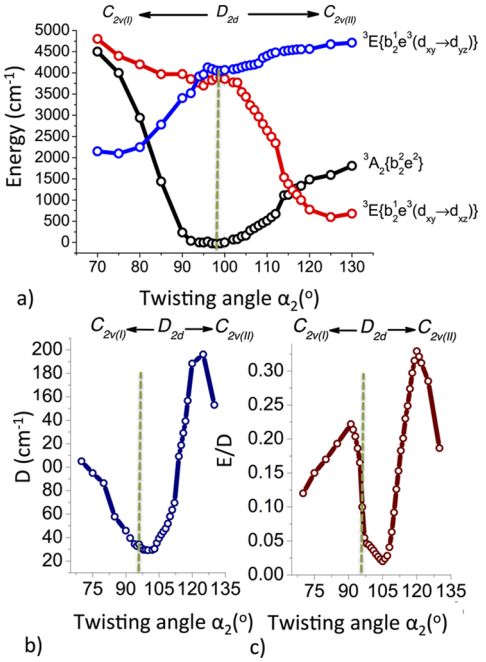

Figure 3. (a) SA-CASSCF/NEVPT2 (12,7) calculated ground-state $^3A_2$ ($b_2^2e^2$) and excited-state $^3E(b_2^1e^3)$, blue and red. Variation of D, dark blue (b) and E/D, dark red (c), along the interconversion pathway $C_{2v(I)} \rightarrow D_{2d} \rightarrow C_{2v(II)}$ for complex **1**. The dashed gray line indicates the crystallographic value of twisting angle $a_2 = 98°$.

around the D_{2d} symmetric structures. Such instability is imposed by the PJT effect of the excited degenerate ^3E ($b_2^1e^3$) states. This is apparently not the case for complex **1**, because the bulky ^{i}Pr groups impose local distortions around the $NiSe_4$ core, lifting the degeneracy of the ^3E ($b_2^1e^3$) states (ΔE = 400 cm^{-1}). Indeed, for twisting angles $90° \leq \alpha_2 \leq 110°$, the ground state is dominated by the $^3A_2$ $b_2^2e^2$ state. Beyond these limits, the $C_{2v(I,II)}$ structures are stabilized, as the ground state is dominated by the $^3E\{b_2^1e^3(d_{xy} \rightarrow d_{xz})\}$ and $^3E\{b_2^1e^3(d_{xy} \rightarrow d_{yz})\}$ states, respectively. It should be stressed, however, that stabilization of these states for this family of complexes requires ligands bearing the same R peripheral groups and/or the presence of coordinating solvents (the latter in pseudo-octahedral complexes). For a complex containing chelating ligands, this is a complicated process, involving rotation of the principal axes system which influences drastically the rhombicity (E/D) of the system (Figure 3c).[17,20,22] In an effort to further correlate the experimentally determined zfs parameters with the anisotropic coordination environment around the Ni^{II} center, the zfs parameters were evaluated along the $C_{2v(I)} \rightarrow D_{2d} \rightarrow C_{2v(II)}$ symmetry-lowering interconversion pathway (Figures 3, S6). As can be seen in Figure 3b, around twisting angles $90° \leq \alpha_2 \leq 110°$, the magnitude of D varies between 30 and 50 cm^{-1}.

It should be also noted that for all these values, the sign of D is well-defined, as E/D dictates axial symmetry with values varying between 0.01 and 0.06 (Figures 3c, S6). In particular, for geometries close to the crystallographic structure (α_2 = 98°), the calculated values (D = 47.9 cm^{-1} and E/D = 0.05) show excellent agreement with experiment (D = 45.40 cm^{-1} and E/D = 0.04). The major contribution to D originates from SOC interactions. In fact, preliminary complete active space configuration interaction calculations provided SSC contributions on the order of 1 cm^{-1}. We can further deconvolute the SOC contributions to D, in terms of contributions from the Ni and Se atoms (see Supporting Information) as well as in terms of state contributions, as shown in Table 1. These data show

Table 1. Atom Type and State Contributions to the Magnitude of D of complex 1, Calculated at the CASSCF(12.7)/NEVPT2 Level

	Contribution to D		
Dominating State	Ni(SOC) (cm^{-1})	Se(SOC) (cm^{-1})	Total (cm^{-1})
$^3E\{b_2^1e^3(d_{xy} \rightarrow d_{yz})\}$	34.9	-5.8	29.1
$^3E\{b_2^1e^3(d_{xy} \rightarrow d_{xz})\}$	38.8	-3	35.8
$^3E\{a_1^1/b_1^1e^3(d_{z2}/d_{x2-y2} \rightarrow d_{yz})\}$	-36.7	5.4	-31.3
$^3E\{a_1^1/b_1^1e^3(d_{z2}/d_{x2-y2} \rightarrow d_{xz})\}$	13.4	-0.05	13.35
D_{SOC}	50.4	-3.4	46.9
D_{SSC}			1.0
D_{total}			47.9
D_{exp}			45.40

that the magnitude of D is dominated by SOC interactions arising mainly from the Ni atom. On the other hand, the ligand SOC originating from the Se donor atoms is one order of magnitude smaller and, moreover, shows opposite sign with respect to the nickel SOC. This is in agreement with recent studies on pseudo-octahedral Ni^{II} complexes bearing chelating (O,E) ligands, E = S, Se, and coordinating solvent molecules, showing negligible effects of Se coordination to the magnitude of D.[17] Nevertheless, additional experimental and computational investigations are needed before any generalization can be made with respect to SOC contributions of Se-containing ligands. Establishing the relative contribution of metal and ligand SOC effects to the magnitude of zfs is of paramount importance. For instance, significant ligand SOC contributions of heavier halides have been established in four-coordinate Ni^{II} complexes.[32]

To get further insight concerning magnetostructural correlations for complex **1**, significant information can be obtained by showing, in the molecular crystallographic frame, the computationally determined x,y,z components of the zfs tensor as well as by further analyzing the contribution to the zfs of the dominant excitations. As can be seen in Figure 1a, the calculated zfs x,y,z components deviate by only 2−3° from the experimentally determined magnetization principal axes. This confirms the misorientation of the latter from the crystallographic axes (*vide supra*).

Furthermore, as discussed above, the dominant contributions to the zfs arise from transitions involving doubly and singly occupied molecular orbitals (DOMO−SOMO). Hence, the $SOMO_S$ determine the magnetic anisotropy of the system. In the absence of covalent bonding interactions between Ni^{II} and the Se donor atoms, the experimentally determined magnetization principal axes would coincide with the crystallographic ones. However, covalency interactions modify the shape and the orientation of the d_{xz} and d_{yz} Ni^{II} orbitals so that they overlap more effectively with the $p_{x,y,z}$ Se orbitals. Hence, the magnetization principal axes are reoriented due to the Ni−Se covalent interactions. These effects merit further investigations by applying more appropriate methodologies, like the ab initio ligand field protocol,[33] which are currently ongoing and will be reported elsewhere.

DOI: 10.1021/jacs.5b06716
J. Am. Chem. Soc. 2015, 137, 12923−12928

CONCLUSION

In conclusion, angle-resolved magnetometry revealed the orientation of the magnetization principal axes in the tetrahedral $Ni^{II}Se_4$-containing complex **1**, confirming its easy-plane anisotropy. First- and second-coordination sphere effects lead to a $^3A_2$ rather than ^3E ground state, and a correspondingly large (45.40 cm^{-1}) zfs D component. The latter was directly determined by FIRMS and computationally shown to be dominated by SOC contributions of the Ni ion and remarkably smaller ones of the Se donor atoms. This work expands the set of paramagnetic systems accessible to FIRMS. Axial (E = 0) complexes of Ni^{II} exhibiting large negative D values, holding promise to behave as mononuclear SMMs, could also be investigated by this method.

ASSOCIATED CONTENT

Supporting Information

The Supporting Information is available free of charge on the ACS Publications website at DOI: 10.1021/jacs.5b06716.

Synthesis of complex **1**, FIRMS, magnetometry, spin Hamiltonian parameters of S = 1 systems, computational details, Scheme 1, Figures S1−S6, references (PDF)

AUTHOR INFORMATION

Corresponding Authors

*Lapo.Bogani@materials.ox.ac.uk
*Frank.Neese@cec.mpg.de
*Kyritsis@chem.uoa.gr

Present Addresses

[⊥]College of Chemistry and Molecular Engineering, Peking University, Beijing 100871, P. R. China
[#]Department of Materials, University of Oxford, 16 Parks Road, OX1 3PH, Oxford, United Kingdom

Author Contributions

[▽]These authors contributed equally.

Notes

The authors declare no competing financial interest.

ACKNOWLEDGMENTS

We thank J. van Slageren for many useful discussions and the reviewers of the manuscript for their constructive comments. This work was supported by the Special Research Account of the University of Athens (N.L., E.F., P.K.), the Max Planck Society (D.M., F.N.) and the Alexander von Humboldt Foundation (S.-D.J., K.T., and L.B.). Part of this work was performed at the National High Magnetic Field Laboratory (NHMFL), funded by National Science Foundation through Cooperative Agreement DMR 1157490, the State of Florida, and the US Department of Energy. P.K. thanks the Fulbright Foundation in Greece and the NHMFL for supporting his recent scientific visit to the latter.

REFERENCES

(1) (a) Gatteschi, D.; Sessoli, R. *Angew. Chem., Int. Ed.* **2003**, *42*, 268. (b) Aromi, G.; Brechin, E. K. In *Single-Molecule Magnets and Related Phenomena*; Winpenny, R., Ed. **2006**; Vol. *122*, p 1 10.1007/430_022. (c) Gatteschi, D.; Bogani, L.; Cornia, A.; Mannini, M.; Sorace, L.; Sessoli, R. *Solid State Sci.* **2008**, *10*, 1701. (d) Bagai, R.; Christou, G. *Chem. Soc. Rev.* **2009**, *38*, 1011.

(2) Neese, F.; Pantazis, D. A. *Faraday Discuss.* **2011**, *148*, 229.

(3) Abragam, A., Bleaney, B. *Electron Paramagnetic Resonance of Transition Ions*; Dover Publications: New York, 1986.

(4) Hill, S.; Datta, S.; Liu, J.; Inglis, R.; Milios, C. J.; Feng, P. L.; Henderson, J. J.; del Barco, E.; Brechin, E. K.; Hendrickson, D. N. *Dalton Trans.* **2010**, *39*, 4693.

(5) (a) Woodruff, D. N.; Winpenny, R. E. P.; Layfield, R. A. *Chem. Rev.* **2013**, *113*, 5110. (b) Meihaus, K. R.; Long, J. R. *Dalton Trans.* **2015**, *44*, 2517.

(6) (a) Craig, G. A.; Murrie, M. *Chem. Soc. Rev.* **2015**, *44*, 2135. (b) Bar, A. K.; Pichon, C.; Sutter, J.-P. *Coord. Chem. Rev.* **2015**, DOI: 10.1016/j.ccr.2015.06.013.

(7) Gatteschi, D.; Barra, A. L.; Caneschi, A.; Cornia, A.; Sessoli, R.; Sorace, L. *Coord. Chem. Rev.* **2006**, *250*, 1514.

(8) Gómez-Coca, S.; Aravena, D.; Morales, R.; Ruiz, E. *Coord. Chem. Rev.* **2015**, *289*, 379.

(9) Atanasov, M.; Aravena, D.; Suturina, E.; Bill, E.; Maganas, D.; Neese, F. *Coord. Chem. Rev.* **2015**, *289*−*290*, 177.

(10) Krzystek, J.; Zvyagin, S. A.; Ozarowski, A.; Trofimenko, S.; Telser, J. *J. Magn. Reson.* **2006**, *178*, 174.

(11) Boča, R. *Coord. Chem. Rev.* **2004**, *248*, 757.

(12) Kowal, A. T.; Zambrano, I. C.; Moura, I.; Moura, J. J. G.; Legall, J.; Johnson, M. K. *Inorg. Chem.* **1988**, *27*, 1162.

(13) (a) van Slageren, J.; Vongtragool, S.; Gorshunov, B.; Mukhin, A. A.; Karl, N.; Krzystek, J.; Telser, J.; Müller, A.; Sangregorio, C.; Gatteschi, D.; Dressel, M. *Phys. Chem. Chem. Phys.* **2003**, *5*, 3837. (b) van Slageren, J.; Vongtragool, S.; Gorshunov, B.; Mukhin, A. A.; Dressel, M. *J. Magn. Magn. Mater.* **2004**, *272*−*276*, E765. (c) van Slageren, J. *Top. Curr. Chem.* **2011**, *321*, 199.

(14) Levesanos, N.; Robertson, S. D.; Maganas, D.; Raptopoulou, C. P.; Terzis, A.; Kyritsis, P.; Chivers, T. *Inorg. Chem.* **2008**, *47*, 2949.

(15) (a) Miklovič, J.; Valigura, D.; Boča, R.; Titič, J. *Dalton Trans.* **2015**, *44*, 12484. (b) Murrie, M.; Marriott, K.; Bhaskaran, L.; Wilson, C.; Medarde, M.; Ochsenbein, S. T.; Hill, S. *Chem. Science* **2015**, DOI: 10.1039/C5SC02854J. (c) Poulten, R. C.; Page, M. J.; Algarra, A. G.; Le Roy, J. J.; López, I.; Carter, E.; Llobet, A.; Macgregor, S. A.; Mahon, M. F.; Murphy, D. M.; Murugesu, M.; Whittlesey, M. K. J. *J. Am. Chem. Soc.* **2013**, *135*, 13640.

(16) (a) Hagen, W. R. *Coord. Chem. Rev.* **1999**, *192*, 209. (b) Krzystek, J.; Ozarowski, A.; Telser, J. *Coord. Chem. Rev.* **2006**, *250*, 2308. (c) Telser, J.; Ozarowski, A.; Krzystek, J. *Electron Paramagnetic Resonance*; Royal Society of Chemistry: Cambridge, U.K., 2012; Vol 23, p 209 10.1039/9781849734837-00209.

(17) Maganas, D.; Krzystek, J.; Ferentinos, E.; Whyte, A. M.; Robertson, N.; Psycharis, V.; Terzis, A.; Neese, F.; Kyritsis, P. *Inorg. Chem.* **2012**, *51*, 7218.

(18) (a) Wojciechowska, A.; Gagor, A.; Duczmal, M.; Staszak, Z.; Ozarowski, A. *Inorg. Chem.* **2013**, *52*, 4360. (b) Schweinfurth, D.; Krzystek, J.; Schapiro, I.; Demeshko, S.; Klein, J.; Telser, J.; Ozarowski, A.; Su, C.-Y.; Meyer, F.; Atanasov, M.; Neese, F.; Sarkar, B. *Inorg. Chem.* **2013**, *52*, 6880. (c) Costes, J. P.; Maurice, R.; Vendier, L. *Chem. - Eur. J.* **2012**, *18*, 4031. (d) Atanasov, M.; Comba, P.; Helmle, S.; Muller, D.; Neese, F. *Inorg. Chem.* **2012**, *51*, 12324. (e) Ruamps, R.; Maurice, R.; Batchelor, L.; Boggio-Pasqua, M.; Guillot, R.; Barra, A. L.; Liu, J.; Bendeif, E.-E.; Pillet, S.; Hill, S.; Mallah, T.; Guihery, N. *J. Am. Chem. Soc.* **2013**, *135*, 3017. (f) Ruamps, R.; Batchelor, L. J.; Maurice, R.; Gogoi, N.; Jimenez-Lozano, P.; Guihery, N.; de Graaf, C.; Barra, A.-L.; Sutter, J.-P.; Mallah, T. *Chem. - Eur. J.* **2013**, *19*, 950. (g) Gómez-Coca, S.; Cremades, E.; Aliaga-Alcalde, N.; Ruiz, E. *Inorg. Chem.* **2014**, *53*, 676. (h) Nemec, I.; Herchel, R.; Svoboda, I.; Boča, R.; Trávniček, Z. *Dalton Trans.* **2015**, *44*, 9551. (i) Wojciechowska, A.; Janczak, J.; Staszak, Z.; Duczmal, M.; Zierkiewicz, W.; Tokar, J.; Ozarowski, A. *New J. Chem.* **2015**, *39*, 6813.

(19) Vanelp, J.; Peng, G.; Searle, B. G.; Mitrakirtley, S.; Huang, Y. H.; Johnson, M. K.; Zhou, Z. H.; Adams, M. W. W.; Maroney, M. J.; Cramer, S. P. *J. Am. Chem. Soc.* **1994**, *116*, 1918.

(20) Maganas, D.; Grigoropoulos, A.; Staniland, S. S.; Chatziefthimiou, S. D.; Harrison, A.; Robertson, N.; Kyritsis, P.; Neese, F. *Inorg. Chem.* **2010**, *49*, 5079.

(21) (a) Davison, A.; Switkes, E. S. *Inorg. Chem.* **1971**, *10*, 837. (b) Bhattacharyya, P.; Novosad, J.; Phillips, J.; Slawin, A. M. Z.; Williams, D. J.; Woollins, J. D. *J. Chem. Soc., Dalton Trans.* **1995**, 1607.

DOI: 10.1021/jacs.5b06716
J. Am. Chem. Soc. 2015, 137, 12923−12928

(c) Rösler, R.; Silvestru, C.; Espinosa-Peréz, G.; Haiduc, I.; Cea-Olivares, R. *Inorg. Chim. Acta* **1996**, *241*, 47.
(22) Ferentinos, E.; Maganas, D.; Raptopoulou, C. P.; Terzis, A.; Psycharis, V.; Robertson, N.; Kyritsis, P. *Dalton Trans.* **2011**, *40*, 169.
(23) (a) Champion, P. M.; Sievers, A. J. *J. Chem. Phys.* **1977**, *66*, 1819. (b) Krzystek, J.; Smirnov, D.; Schlegel, C.; van Slageren, J.; Telser, J.; Ozarowski, A. *J. Magn. Reson.* **2011**, *213*, 158. (c) Telser, J.; van Slageren, J.; Vongtragool, S.; Dressel, M.; Reiff, W. M.; Zvyagin, S. A.; Ozarowski, A.; Krzystek, J. *Magn. Reson. Chem.* **2005**, *43*, S130. (d) Champion, P. M.; Sievers, A. J. *J. Chem. Phys.* **1980**, *72*, 1569.
(24) (a) Vongtragool, S.; Gorshunov, B.; Mukhin, A. A.; van Slageren, J.; Dressel, M.; Müller, A. *Phys. Chem. Chem. Phys.* **2003**, *5*, 2778. (b) Kirchner, N.; van Slageren, J.; Dressel, M. *Inorg. Chim. Acta* **2007**, *360*, 3813. (c) El Hallak, F.; van Slageren, J.; Gómez-Segura, J.; Ruiz-Molina, D.; Dressel, M. *Phys. Rev. B: Condens. Matter Mater. Phys.* **2007**, *75*, 104403. (d) Pieper, O.; Guidi, T.; Carretta, S.; van Slageren, J.; El Hallak, F.; Lake, B.; Santini, P.; Amoretti, G.; Mutka, H.; Koza, M.; Russina, M.; Schnegg, A.; Milios, C. J.; Brechin, E. K.; Julia, A.; Tejada, J. *Phys. Rev. B: Condens. Matter Mater. Phys.* **2010**, *81*, 174420. (e) Moro, F.; Piga, F.; Krivokapic, I.; Burgess, A.; Lewis, W.; McMaster, J.; van Slageren, J. *Inorg. Chim. Acta* **2010**, *363*, 4329. (f) Haas, S.; Heintze, E.; Zapf, S.; Gorshunov, B.; Dressel, M.; Bogani, L. *Phys. Rev. B: Condens. Matter Mater. Phys.* **2014**, *89*, 174409. (g) Marx, R.; Moro, F.; Dörfel, M.; Ungur, L.; Waters, M.; Jiang, S. D.; Orlita, M.; Taylor, J.; Frey, W.; Chibotaru, L. F.; van Slageren, J. *Chem. Science* **2014**, *5*, 3287. (h) Mukhin, A. A.; Travkin, V. D.; Zvezdin, A. K.; Lebedev, S. P.; Caneschi, A.; Gatteschi, D. *Europhys. Lett.* **1998**, *44*, 778.
(25) Li, S.; Hamrick, Y. M.; Van Zee, R. J.; Weltner, W. *J. Am. Chem. Soc.* **1992**, *114*, 4433.
(26) Vongtragool, S.; Gorshunov, B.; Dressel, M.; Krzystek, J.; Eichhorn, D. M.; Telser, J. *Inorg. Chem.* **2003**, *42*, 1788.
(27) Rogez, G.; Rebilly, J. N.; Barra, A. L.; Sorace, L.; Blondin, G.; Kirchner, N.; Duran, M.; van Slageren, J.; Parsons, S.; Ricard, L.; Marvilliers, A.; Mallah, T. *Angew. Chem., Int. Ed.* **2005**, *44*, 1876.
(28) Rebilly, J. N.; Charron, G.; Riviere, E.; Guillot, R.; Barra, A. L.; Serrano, M. D.; van Slageren, J.; Mallah, T. *Chem. - Eur. J.* **2008**, *14*, 1169.
(29) (a) Schnegg, A.; Behrends, J.; Lips, K.; Bittl, R.; Holldack, K. *Phys. Chem. Chem. Phys.* **2009**, *11*, 6820. (b) Dreiser, J.; Schnegg, A.; Holldack, K.; Pedersen, K. S.; Schau-Magnussen, M.; Nehrkorn, J.; Tregenna-Piggott, P.; Mutka, H.; Weihe, H.; Bendix, J.; Waldmann, O. *Chem. - Eur. J.* **2011**, *17*, 7492. (c) Pedersen, K. S.; Dreiser, J.; Nehrkorn, J.; Gysler, M.; Schau-Magnussen, M.; Schnegg, A.; Holldack, K.; Bittl, R.; Piligkos, S.; Weihe, H.; Tregenna-Piggott, P.; Waldmann, O.; Bendix, J. *Chem. Commun.* **2011**, *47*, 6918. (d) Nehrkorn, J.; Martins, B. M.; Holldack, K.; Stoll, S.; Dobbek, H.; Bittl, R.; Schnegg, A. *Mol. Phys.* **2013**, *111*, 2696. (e) Dreiser, J.; Pedersen, K. S.; Schnegg, A.; Holldack, K.; Nehrkorn, J.; Sigrist, M.; Tregenna-Piggott, P.; Mutka, H.; Weihe, H.; Mironov, V. S.; Bendix, J.; Waldmann, O. *Chem. - Eur. J.* **2013**, *19*, 3693. (f) Forshaw, A. P.; Smith, J. M.; Ozarowski, A.; Krzystek, J.; Smirnov, D.; Zvyagin, S. A.; Harris, T. D.; Karunadasa, H. I.; Zadrozny, J. M.; Schnegg, A.; Holldack, K.; Jackson, T. A.; Alamiri, A.; Barnes, D. M.; Telser, J. *Inorg. Chem.* **2013**, *52*, 144.
(30) (a) Jiang, S.-D.; Wang, B.-W.; Gao, S. *Struct. Bonding (Berlin, Ger.)* **2014**, *164*, 111. (b) Luzon, X.; Sessoli, R. *Dalton Trans.* **2012**, *41*, 13556.
(31) Maganas, D.; Sottini, S.; Kyritsis, P.; Groenen, E. J. J.; Neese, F. *Inorg. Chem.* **2011**, *50*, 8741.
(32) (a) Atanasov, M.; Rauzy, C.; Baettig, P.; Daul, C. *Int. J. Quantum Chem.* **2005**, *102*, 119. (b) Ye, S.; Neese, F. *J. Chem. Theory Comput.* **2012**, *8*, 2344.
(33) (a) Atanasov, M.; Ganyushin, D.; Sivalingam, K.; Neese, F. *Struct. Bonding (Berlin, Ger.)* **2011**, *143*, 149. (b) Atanasov, M.; Zadrozny, J. M.; Long, J. R.; Neese, F. *Chem. Science* **2013**, *4*, 139.

DOI: 10.1021/jacs.5b06716
J. Am. Chem. Soc. 2015, 137, 12923−12928